STEM PROBE SPREADING

L.D. MARKS
Department of Physics, Arizona State University, Tempe, AZ 85287

ABSTRACT

The theoretical ideas for STEM probe spreading using spherical wave X-ray diffraction theory and experimental results of diffractive probe spreading are briefly described. Clear evidence is found for two beam Bormann fan effects arising from high order diffracted beams.

INTRODUCTION

One of the growing areas of application of electron microscopy in materials science is microanalysis. By using the elementary characteristic loss processes of a swift (100keV) electron probe propogating through the specimen, local chemical compositions can be determined. In particular, important information about, for instance, the nature and extent of any grain boundary segregation can be obtained. In order to quantify the experimental results, it is essential to know what is the volume of the specimen which the electron probe sees, in particular the transverse spreading perpendicular to the incident probe direction. If this transverse spreading is small, for instance 5Å, segregation as a function of distance from a boundary can be determined to a high accuracy. If it is large, say 100Å, then some form of deconvolution procedure is the only route to detailed information.

Over the last few years a number of authors have investigated the probe spreading in a STEM theoretically (e.g. [1-4] and the references therein). All these theories have employed a ballistic model for the electrons, i.e. classical hard particles which have a certain probability of being scattered as a function of distance. However, electrons need to be treated Quantum Mechanically, rather than by a ballistic model. For instance, ballistic models fail to represent diffraction correctly which is frequently the dominant scattering process for swift electrons.

In this paper we deal with an improved analysis of the STEM probe spreading based upon spherical wave X-ray diffraction theory (e.g. [5-8]), and show experimental results which clearly show the diffractive spreading. Preliminary reports of the theory [9] and experimental results [10] have been presented elsewhere, and more detailed descriptions of the theory, STEM probe spreading and experimental results are being prepared.

DIFFRACTION THEORY

In this section we will briefly sketch the main theoretical ideas for describing the STEM probe spreading.

Within a specimen, the electron wave $\psi(\underline{r})$ can be expressed in terms of Bloch waves, i.e.

$$\psi(\underline{r}) = \sum_j \int A_j(\underline{k}_j)\, B(\underline{r},\underline{k}_j) d^2\underline{k}_j \qquad -1$$

where $B_j(\underline{r},\underline{k}_j)$ is a Bloch wave of form:

$$B_j(\underline{r},\underline{k}_j) = \exp(2\pi i \underline{k}_j.\underline{r}) \sum_{\underline{g}} C_{\underline{g}} \exp(2\pi i \underline{g}.\underline{r}) \qquad -2$$

and $A_j(\underline{k}_j)$ is determine by matching at the entrance surface of the specimen. A number of "j" levels are occupied, typically two to five. The integral form of equation 1 arises when we have an incident wavepacket as in a STEM instrument. We note that the integral in equation 1 is to be performed over the dispersion surface.

In general the wave propogation can be described by optical techniques.

Mat. Res. Soc. Symp. Proc. Vol. 41. © 1985 Materials Research Society

Following Kato [11], each Bloch wavepacket is expanded by an optical anzatz

$$\int A_j(\underline{k}_j)B_j(\underline{r}_j\underline{k}_j)d^2\underline{k}_j = D_j(\underline{r})\exp(iS_j(\underline{r})) \qquad -3$$

leading to a wavepacket which propogates along the direction normal to the dispersion surface. Each of the branches propogate in general in different directions, as illustrated in Figure 1.

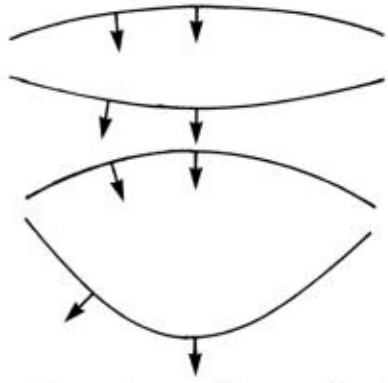

Figure 1 Dispersion surface for high energy electrons, with the propogation directions for two different directions arrowed.

The precise results are quite strongly dependant upon the orientation of the material, the structure and the strength of the scattering. For most materials at a zone axis the dispersion surface is quite flat. By analogy with solid-state theory we can describe the material as tightly-bound. Here the probe spreading is small with the electron wave channelling down the atomic columns, as shown in Figure 2.

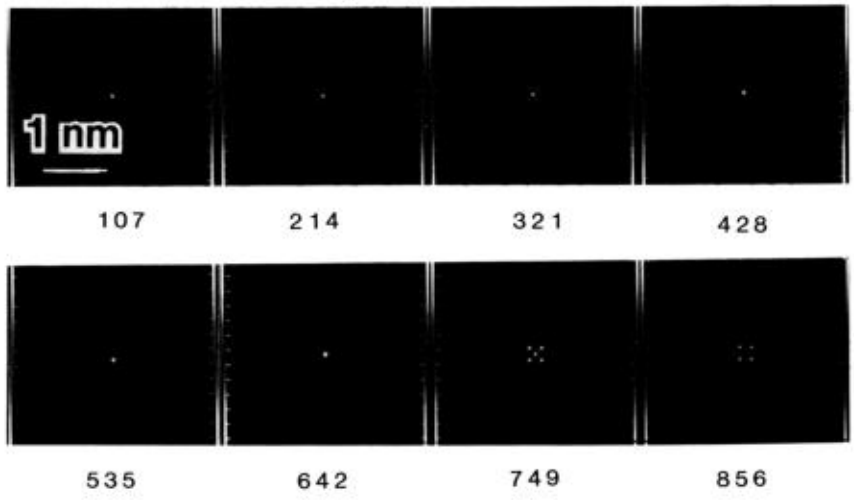

Figure 2 The shape of a probe calculated by a multislice analysis, initially about 3Å (i.e. for a VG STEM instrument) as a function of thickness through a diamond specimen on a <100> zone axis. The probe remains small, particularly by comparison with the later Figures. The thicknesses in angstroms are marked.

Away from the zone axis, and in particular when the central orientation of the probe is near to a kinematical orientation or near the Brillouin zone boundary of the projected two dimensional structure the spreading of the probe is far larger, an example being shown in Figure 3.

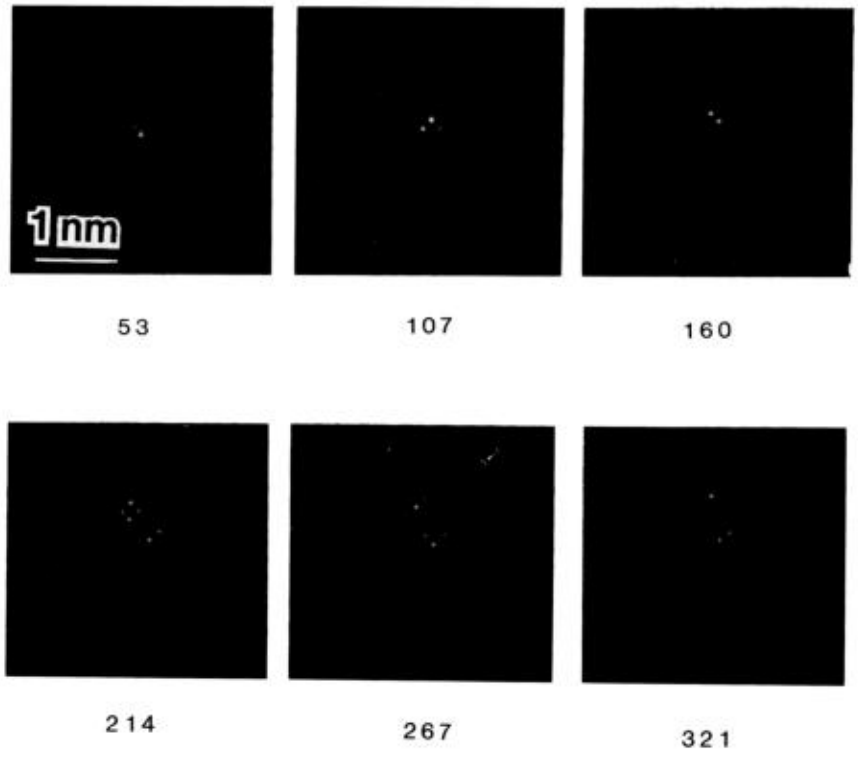

Figure 3 The shape of a probe near a Brillouin zone orientation for diamond (100). The thicknesses are shown on the Figures. The same algorithm and initial conditions were used as for Figure 2. The substantially larger spreading should be noted.

In many cases, and in particular for our purposes herein, we only need to consider two "j" branches, the standard two beam approximation. The solution for this case was first given by Kato [12], and grew out of the X-ray topography experiments of Kato and Lang [13]. For an incident delta function on the specimen, the diffracted beam amplitude is

$$\phi_g(\underline{\rho},z) = \frac{2\pi i}{\varepsilon_g} F(\underline{\rho},z) \qquad -4$$

where $F(\underline{\rho},z) = J_o[\frac{1}{\lambda g \varepsilon_g}[(\lambda g z/2)^2 - \rho^2]^{1/2}]$ $\quad 2|\underline{\rho}| < \lambda g z,\ \underline{\rho}\cdot\underline{g} = 0$

$= 0$ $\quad 2|\underline{\rho}| > \lambda g z$ or $\underline{\rho}\cdot\underline{g} \neq 0$ $\qquad -5$

whilst the transmitted beam amplitude is

$$\phi_o(\underline{\rho},z) = 2\partial F/\partial z + \lambda g \partial F/\partial \rho \qquad -6$$

where the total electron wave is

$$\psi(\underline{r}) = [\ \phi_o(\underline{\rho},z) + \phi_g(\underline{\rho},z)\exp(2\pi i\underline{g}.\underline{r})]\exp(2\pi i\underline{k}.\underline{r}) \qquad -7$$

and the incident wave at the entrance surface is

$$\psi(\underline{r}) = \int \exp(2\pi i\underline{k}.\underline{r})d^2\underline{k} \qquad -8$$

z being the beam direction, $\underline{\rho}$ in the plane normal to z. The intensity of both the transmitted and diffracted beams span a Borrmann fan along $\underline{g}$ of width λgz. The propogation of both beams together through the specimen in the same direction is one of the main differences between Quantum Mechanical and classical electrons - for a classical model the diffracted beam propogates in a different direction to the transmitted wave. For a non delta function incident wave, we can (approximately) convolve the result by the form of the incident probe. With a more realistic incident probe and diffracting conditions the result is more complicated, but the main result of a diffractive streak along $\underline{g}$ remains valid.

EXPERIMENTAL PROCEDURE

Experiments were performed in a Philips 400 T FEG electron microscope. In nanoprobe mode, a probe can be produced of order 20Å in diameter and imaged straightforwardly in TEM mode at high magnifications. The specimens used were <111> oriented silicon single crystals, chemically thinned and cleaned by standard semiconductor solvents immediately before use. The latter both reduced contamination problems and reduced the amorphous SiO_2 coverage to a thickness of 10-20Å (determined by high resolution electron microscopy). To further reduce contamination, the specimens were cooled to liquid nitrogen temperatures. The thickness of the specimens were determined from the two beam microdiffraction patterns around the (440) spots (in Figure 4).

EXPERIMENTAL RESULTS

One problem with detecting the diffractive probe spreading is that the effects from low order diffracted beams is small, of order λgz. Furthermore, λgz is an upper limit for nearly free electron Bloch waves whilst most materials at 100kV are quite tightly bound. (The spreading for tightly bound levels is substantially smaller since the dispersion surfaces are relatively flat.) Therefore to experimentally detect the spreading due to low order beams a substantially smaller incident probe would be required.

What could in practise be readily observed were effects from higher order spots - with a large converence angle it is essentially impossible to avoid exciting "stray" spots. A series of images showing the diffractive streaks from these high order spots for different thicknesses are shown in Figure 4, with a multislice calculation of the probe shape for a similar and thickness and diffraction condition also shown in the Figure. The experimental and calculated images are with an objective aperture around the central beam to minimise effects from the post specimen lenses. Therefore the fine detail in Figures 2 and 3 (due to coherent lattice fringes associated with the diffracted beams) is missing.

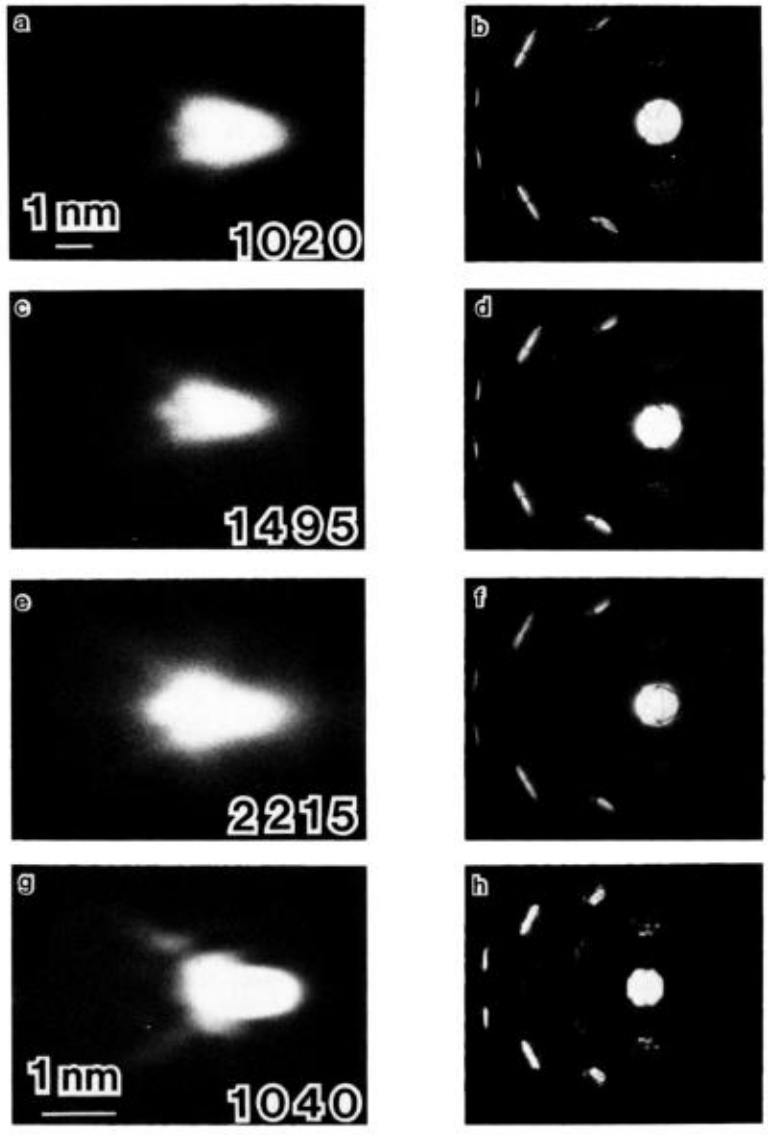

Figure 4 Experimental results for the probe spreading, image and diffraction patterns across the page with the thickness increasing down the page. The legs on the probe are due to Borrmann streaks with (440) beams. Numerical calculations for the probe shape and the microdiffraction pattern are shown in g) and h), with the specimen thicknesses in Angstroms marked on the Figure.

DISCUSSION

The agreement between the theoretical prediction of diffractive streaks and the experimental results is quite encouraging. The qualitative agreement between the experimental results and the calculation of Figure 4 confirm that the probe spreading is a Quantum Mechanical diffractive phenomenum. The correspondence between the diffraction patterns in b) and h) of this Figure is exceedingly good. The main difference at present between the theory and experiment is the central region in a) and g). This will be sensitive to the incoherence of the incident probe, and further work is required to develop models for partially coherent probes. There may be additional complications arising from inelastic scattering, which have been avoided by using silicon specimens. (Silicon has very little phonon scattering, particularly at liquid nitrogen temperatures, whilst as pointed out by Howie [14], plasmon scattering only introduces primarily an energy spread rather than any transverse spreading.) A ballistic analysis will certainly not reproduce the experimental results. Unfortunately we must also abandon the simple analytical elegance of ballistic theories of the probe spreading - as is well known, diffraction is very structure and orientation dependant and not simply a function of mass density and thickness. It may prove to be necessary to perform detailed numerical calculations for each specimen and orientation, as is now standard for high resolution imaging. Fortunately there are some simplifications. As mentioned earlier, the probe is far smaller for a tightly bound potential. In particular, zone axis orientations for quite heavy and dense materials are tightly bound. This will be one route to obtaining accurate local analytical information. This orientation dependance will be discussed in more detail elsewhere.

ACKNOWLEDGMENTS

The author would like to thank Professors, J.M. Cowley and R. Carpenter for advice and disucssion. This work was funded on Department of Energy Grant No. DE-AC02-76ER02995.

REFERENCES

1. J.I. Goldstein, J.L. Costley, G.W. Lorimer and S.J. Reed, SEM/1977, Ed. O. Johari (IITRI, Chicago, IL) 315.
2. R.G. Faulkner and K. Norgaard, X-ray Spectrometry 7, 181 (1978).
3. P. Doing, D. Lonsdale and P.E.J. Flewitt, Phil. Mag. A41, 761 (1980).
4. P. Rez, Ultramicroscopy 12, 29 (1983).
5. L.V. Azaroff, R. Kaplow, N. Kato, R.L. Weiss, A.J.C. Wilson and R.A. Young, X-ray Diffraction (McGraw-Hill, New York, 1974).
6. M. Hart, in Characterisation of Crystal Growth Defects by X-ray Methods, Ed. Tanner and Bowen (Plenum Press, New York, (1980) p. 216.
7. N. Kato, ibid, p. 264.
8. Z.G. Pinsker, Dynamical Scattering of X-rays in Crystals (Springer-Verlag, New York, 1978).
9. L.D. Marks, in Proceedings Eight European Congress on Electron Microscopy EDS Csanady, Rohlich and Szabo, p. 137, 1984.
10. L.D. Marks, submitted to Ultramicroscopy, 1984.
11. N. Kato, Acta. Cryst. A24, 157 (1968).
12. N. Kato, Acta. Cryst. 14 526 (1961) and 14 627 (1961).
13. N. Kato and A.R. Lang, Acta Cryst. 12, 787 (1959).
14. A. Howie, Proc. Roy. Soc. A271, 268 (1963).